Chen-Hu, K., Alexandropoulos, G. C. & García Armada, A. (4-8 December 2022). *Simultaneous RIS Tuning and Differential Data Transmission for MISO OFDM Wireless Systems* [proceedings]. GLOBECOM 2022 - 2022 IEEE Global Communications Conference, Rio de Janeiro, Brazil.

DOI: 10.1109/GLOBECOM48099.2022.10000904

Simultaneous RIS Tuning and Differential Data Transmission for MISO OFDM Wireless Systems

Kun Chen-Hu[1], George C. Alexandropoulos[2,3], and Ana García Armada[1]
[1]Department of Signal Theory and Communications, Universidad Carlos III de Madrid, Spain
[2]Department of Informatics and Telecommunications, National and Kapodistrian University of Athens, Greece
[3]Technology Innovation Institute, 9639 Masdar City, Abu Dhabi, United Arab Emirates
E-mails: kchen@tsc.uc3m.es, alexandg@di.uoa.gr, agarcia@tsc.uc3m.es

***Abstract*—The Reconfigurable Intelligent Surfaces (RIS) constitute one of the prominent technologies for the next generation of wireless communications. They are mainly envisioned to efficiently enhance the signal coverage in cases where the direct communication link is weak or obstructed. Recently, beam training based on codebook selection has been proposed as a low-latency means for tuning the RIS phase profile according to a desired performance metric. However, it requires the transmission of reference signals to measure the performance with different RIS phase configurations available in the codebook, which reduces the spectral efficiency. In this paper, we consider the uplink of a Multiple-Input Signal-Output (MISO) communication system with Orthogonal Frequency-Division Multiplexing (OFDM) and present a novel scheme for simultaneous RIS phase configuration and data transmission. The proposed scheme is based on non-coherent differential modulation, which is deployed both in the beam training and the data transmission phases. In the former phase, it also enables energy measurement for the determination of the best RIS phase profile. Then, in the latter phase, a higher throughput can be established through the high gain reflective link. Our numerical results showcase that our proposal can double the system throughput with lower complexity, as compared to the generic state-of-the-art approach.**

***Index Terms*—Beam training, differential modulation, non-coherent communications, reconfigurable intelligent surfaces.**

I. Introduction

Reconfigurable Intelligent Surface (RIS) [1]–[4] is expected to play a significant role in the evolution of mobile communication systems towards the 6-th Generation (6G) [5]. The high frequency bands will be extensively exploited for mobile communications [6], such as 3.5 GHz and millimetre waves (mm-Wave), in order to take advantage of the huge available bandwidth. RIS-empowered links is an appealing solution to both improving and extending the signal transmitted by either the Base Station (BS) or User Equipment (UE), without excessively increasing the overall cost of the wireless network.

The exploitation of RISs requires to obtain a proper phase configuration, capable of creating an alternative high-gain reflective channel between BS and UE [7]–[12]. For that purpose, a significant amount of reference signals is transmitted in the uplink to obtain the so-called cascaded channel estimation, which encompasses the joint effect of the signal propagation over the BS-RIS and RIS-UE links [7]–[9]. Additionally it is absolutely useless when the cascaded channel has a strong attenuation due to the multiplicative fading effects [13]. Given the channel estimation, the best pair of precoder/combiner and phase configuration are computed and communicated to the RIS via a side control link. This processing task is not straightforward due to the fact that a non-convex design optimization needs to be solved, increasing the operational complexity. Several studies have focused on accelerating this optimization at the expense of sacrificing the performance with sub-optimal optimizations [1], [4], [10], [11], [14]. After the RIS is adequately configured, the traditional Coherent Demodulation Scheme (CDS) is used for the data transmission. It is generally assumed that the channel coherence time is long enough to encompass the estimation, optimization, and data transmission, a condition that may be difficult to satisfy, especially in mobile communication systems.

Recently, different alternatives have been proposed in order to alleviate the overhead incurred by the cascaded channel estimation and reduce the delay induced by the optimization, including beam training [15], [16] and the exploitation of the diversity gain of the RIS [17], [18]. The former approaches [15], [16] use codebooks based on a reduced number of phase configurations. Similarly to the beam training proposed for mm-Wave [19], the UE transmits some reference signals and the BS measures the received signal strength when each codeword is applied. The chosen codeword is that one associated with the highest received energy. However, it still requires a beam training period to test all the phase configurations of the codebook. On the other hand, the strategies in [17], [18] assumed that the phase configurations at the RIS are randomly chosen over time, and hence, the received signal will be enhanced due to the time and/or spatial diversity. However, [17] only provides some theoretical bounds of the proposed system. In turn, [18] proposed the use of Non-CDS (NCDS) [20]–[23] capable of avoiding the transmission of reference signals and only exploiting the spatial diversity produced by both the BS and RIS. Although the average performance is scaled by the spatial diversity produced by both the antennas of the BS and the passive elements of the RIS, the received signal may suffer from strong fading for certain periods.

To the best knowledge of the authors, the combination of beam training [15], [16] and NCDS [20]–[23] for RIS-aided communications has never been proposed. In this paper, we propose the simultaneous beam training procedure and data

978-1-6654-3540-6/22

transmission based on differential encoding. During the beam training process, the effective BS-UE channel is strongly time-varying as a consequence of testing different phase configurations of the RIS profile codebook. However, data transmission can be efficiently performed during those training periods by using NCDS, which allows to both measure the received energy for each chosen codeword and demodulate the received signals without the knowledge of the channel estimation. Unlike CDS, it is very robust to the time variability. Hence, the best codeword can be selected without sacrificing the data-rate. Moreover, after the alternative link between BS and UE via RIS has been established, the NCDS is still a preferable choice as compared to the traditional CDS, as will be shown. For high mobility scenarios where the channel coherence time may be small, the NCDS is able to fully avoid the estimation of the resulting channel between BS-UE, and hence, the data-rate is increased. Also in this transmission stage, computing the precoder/combiner at the BS is not required, reducing the complexity, delay and energy consumption of the system, as will be shown in the numerical results.

Notation: Matrices, vectors, and scalar quantities are denoted by boldface uppercase, boldface lowercase, and normal letters, respectively. $[\mathbf{A}]_{mn}$ denotes the element in the m-th row and n-th column of $\mathbf{A}$. $\jmath$ is the imaginary unit, $|\cdot|$ represents the absolute value and $\measuredangle(\cdot)$ corresponds to the phase component of a complex number. $\mathcal{CN}(0,\sigma^2)$ represents the circularly-symmetric and zero-mean complex normal distribution with variance σ^2.

II. System Model

The considered mobile Multiple-Input Signal-Output (MISO) communications scenario comprises a BS, an RIS, and a single-antenna UE. The BS is equipped with a uniform rectangular array (URA) consisting of $B = B_H B_V$ antenna elements, where B_H and B_V denote the number of elements in the horizontal and vertical axes, respectively, and the distance between any two contiguous elements in their respective axes is given by d_H^{BS} and d_V^{BS}. Analogously to the BS, the RIS is built by $M = M_H M_V$ fully passive reflecting elements, whose respective distances between elements are given by d_H^{RIS} and d_V^{RIS}. We finally assume that the RIS is attached to a dedicated controller for managing its configuration, which is synchronized with the BS.

Focusing on the uplink case, the UE transmits the data to the BS using both the direct BS-UE link and the reflected link via the BS-RIS and RIS-UE communication links. It is understood that other UEs may be multiplexed in different orthogonal (e.g. time or frequency) resources. Given the channel coherence time (T_c), the UE transmits a frame of N contiguous Orthogonal Frequency-Division Multiplexing (OFDM) symbols of K subcarriers each. In order to avoid the Inter-Symbol and Inter-Carrier Interferences (ISI and ICI), the length L_{CP} of the cyclic prefix must be long enough to absorb the BS-UE direct and reflective paths. At the BS, the baseband representation of the received signal $\mathbf{y}_{k,n} \in \mathbb{C}^B$ at the k-th subcarrier in the n-th OFDM symbol is given by

$$\mathbf{y}_{k,n} = \mathbf{h}_{k,n} x_{k,n} + \mathbf{v}_{k,n}, \quad 1 \le k \le K, \quad 1 \le n \le N, \tag{1}$$

where $x_{k,n} \in \mathbb{C}$ denotes the complex symbol transmitted from the UE whose power is $\mathbb{E}\{|x|^2\} = P_x$, $\mathbf{v}_{k,n} \in \mathbb{C}^B$ represents the Additive White Gaussian Noise (AWGN) vector which is distributed as $[\mathbf{v}_{k,n}]_b \sim \mathcal{CN}(0,\sigma_v^2)$, and $\mathbf{h}_{k,n} \in \mathbb{C}^B$ is the effective channel frequency response between BS and UE, which can be decomposed as

$$\mathbf{h}_{k,n} \triangleq \mathbf{h}_{d,k} + \mathbf{h}_{r,k,n} = \mathbf{h}_{d,k} + \mathbf{H}_{q,k}\boldsymbol{\psi}_n, \tag{2}$$
$$1 \le k \le K, \quad 1 \le n \le N,$$

where $\mathbf{h}_{d,k} \in \mathbb{C}^B$ is the direct BS-UE channel frequency response at the k-th subcarrier, $\mathbf{h}_{r,k,n} \in \mathbb{C}^B$ corresponds to the reflective BS-UE channel frequency response through the RIS at the k-th subcarrier in the n-th OFDM symbol. The symbol $\boldsymbol{\psi}_n \in \mathbb{C}^M$ accounts for the phase configurations applied to the RIS at the n-th OFDM symbol, which is defined as

$$\boldsymbol{\psi}_n \triangleq \left[\exp(\jmath\psi_{n,1}) \quad \cdots \quad \exp(\jmath\psi_{n,M})\right]^T, \quad 1 \le n \le N, \tag{3}$$

with $\psi_{n,m}$ for $1 \le m \le M$ representing the m-th phase shift of the RIS. $\mathbf{H}_{q,k} \in \mathbb{C}^{B\times M}$ denotes the cascaded channel frequency response at k-th subcarrier which is given by

$$[\mathbf{H}_{q,k}]_{b,m} = [\mathbf{G}_{e,k}]_{b,m}\,[\mathbf{g}_{u,k}]_m, \tag{4}$$
$$1 \le k \le K, \quad 1 \le b \le B, \quad 1 \le m \le M,$$

where $\mathbf{G}_{e,k}$ and $\mathbf{g}_{u,k}$ are the channel frequency response of the BS-RIS and RIS-UE links, respectively, at the k-th subcarrier.

III. NCDS based on Differential Modulation

The beam training process [15], [16] relies on the transmission of reference signals in order to allow to measure the received energy. Furthermore, once the best beam of the codebook is chosen, the data symbols are transmitted and received by using the classical CDS, which also relies on reference signals. Consequently, in order to successfully deploy an RIS-empowered communication system, the transmission of a significant amount of overhead is required, which implies a reduction of the efficiency of the system, especially for high mobility scenarios where the required amount of pilot symbols is much larger.

The proposal of exploiting NCDS based on differential modulation [20]–[23] at RIS-aided communications during and after the beam training process is presented in this section (see Fig. 1). The N OFDM symbols transmitted during the channel coherence time (T_c) are split into the two stages (see Fig. 1). In the first stage, N_l OFDM symbols are transmitted from the UE to the BS through the direct link, and at the same time, the panel will test different phase configurations given by the codebook. In the second stage, the remaining N_h OFDM symbols are transmitted by mainly using the enhanced reflected link, thanks for the selection of the best phase configuration of the codebook for the RIS. Consequently, at

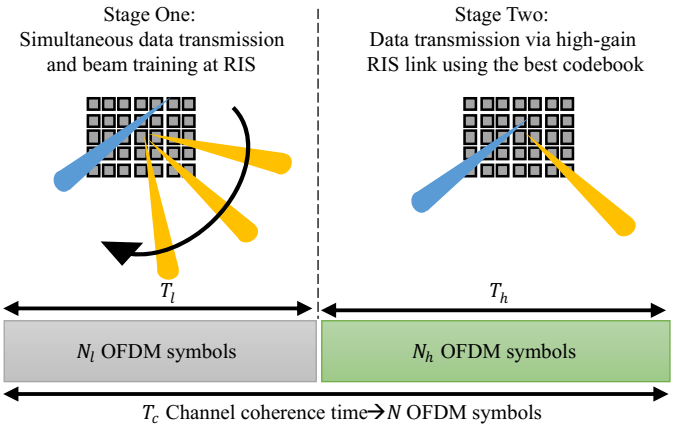

Fig. 1. A frame of N OFDM symbols is transmitted by two stages within the channel coherence time (T_c). In the first stage, beam training is executed, and at the same time, non-coherent transmission is performed over the BS-UE direct link. In the second stage, the best phase configuration is loaded to the RIS and non-coherent data symbols are transmitted over the enhanced reflective BS-UE link via RIS.

the second stage, the communication link via RIS provides a higher gain than the direct link, and higher order modulations can be exploited, producing a better throughput.

A. Stage One: Simultaneous Data Transmission and Beam Training at the RIS

The beam training is performed over the first consecutive N_l OFDM symbols, where each entry of the codebook is configured at the RIS for, at least, the duration of one OFDM symbol ($N_l \geq N_{CB}$). At this stage, even though all the channel links remain invariant during the channel coherence time (T_c), the effective BS-UE channel ($\mathbf{h}_{k,n}$), given in (2), is different from one to the following OFDM symbol. This effect is produced by the reflective link ($\mathbf{h}_{r,k,n}$), which is constantly varying as a consequence of using different codewords (ψ_n) at each OFDM symbol. In order to be able to transmit data during this training period, the differential modulation is performed between consecutive subcarriers, in particular, we deploy the Frequency-Domain Scheme (FDS) of [21].

At the UE, the data symbols are differentially encoded in the frequency domain before their transmission as follows:

$$x_{k,n} = \begin{cases} p_{k,n}, & k = 1 \\ x_{k-1,n} p_{k,n}, & k = 2 \\ x_{k-1,n} s_{k,n}, & 3 \leq k \leq K \end{cases}, \quad 1 \leq n \leq N. \tag{5}$$

where $s_{k,n}$ denotes the complex symbol to be transmitted at the k-th subcarrier and the n-th OFDM symbol, that belongs to a Q_l-PSK constellation and its power is normalized (i.e., $|s_{k,n}|^2 = 1$). The constellation size at this stage may be small since the direct BS-UE channel link does not have a LoS component and the path-loss may be high. In (5), $p_{1,n}$ and $p_{2,n}$ are two reference symbols. Before data transmission, the power of differential symbols x_k^n is scaled according to P_x.

According to [21], [23], the differential modulation performed at FDS is chosen when the channel coherence time is reduced to up to one OFDM symbol period ($T_c \approx (K + L_{CP})/(K\Delta f)$ with Δf being the subcarrier spacing measured in Hz), where the data symbols are differentially encoded in the contiguous frequency resources of each OFDM symbol. However, this scheme requires two reference symbols ($p_{1,n}$ and $p_{2,n}$), namely the first one to estimate and compensate the residual differential phase component ($\zeta_{l,n}$) produced by the multi-path channel at the n-th OFDM symbol at the first stage, and the second one for performing the differential demodulation. Note that this overhead can be neglected for broadband systems, when K is very large.

Given the received signal (1), the BS performs the following differential decoding:

$$z_{k,n} = \frac{1}{B} \left(\mathbf{y}_{k-1,n}\right)^H \mathbf{y}_{k,n} \exp\left(-\jmath \widehat{\zeta}_{l,n}\right) = \frac{1}{B} \exp\left(-\jmath \widehat{\zeta}_{l,n}\right) \sum_{i=1}^{4} I_i, \tag{6}$$

$$I_1 = \left(\mathbf{h}_{k-1,n}\right)^H \mathbf{h}_{k,n} s_{k,n}, \quad I_2 = \left(\mathbf{h}_{k-1,n} x_{k-1,n}\right)^H \mathbf{v}_{k,n}, \tag{7}$$

$$I_3 = \left(\mathbf{v}_{k-1,n}\right)^H \mathbf{h}_{k,n} x_{k,n}, \quad I_4 = \left(\mathbf{v}_{k-1,n}\right)^H \mathbf{v}_{k,n}, \tag{8}$$

$$3 \leq k \leq K, \quad 1 \leq n \leq N,$$

where I_1 includes the useful symbol $s_{k,n}$, I_2 and I_3 represent the cross-interference terms produced by the noise and the received differential symbol in two time instants, while I_4 is exclusively produced by the product of the noise in two contiguous subcarriers. Moreover, the residual phase component at the n-th OFDM symbol can be estimated as

$$\widehat{\zeta}_{l,n} = \measuredangle\left(\left(\mathbf{y}_{1,n}\right)^H \mathbf{y}_{2,n}\right) - \measuredangle\left(\frac{p_{2,n}}{p_{1,n}}\right), \quad 1 \leq n \leq N. \tag{9}$$

While this transmission occurs, the beam training process is being executed at the RIS, where a different phase configuration of the codebook is configured for each group of N_l consecutive OFDM symbols, and the BS is measuring the received power in the n-OFDM symbol as follows:

$$P_{y,n} = \frac{1}{K} \sum_{k=1}^{k} \left|\mathbf{y}_{k,n}\right|^2, \quad 1 \leq n \leq N_l. \tag{10}$$

After testing all entries of the codebook, the BS will choose that phase configuration corresponding to the highest measured received power (10). Hence, the gain of the reflective channel is significantly enhanced by the RIS.

B. Stage Two: Data Transmission via Reflective RIS Link

Once the best phase configuration is chosen in the previous stage, the effective BS-UE channel remains constant for N_h OFDM symbols ($\mathbf{h}_{k,n} = \mathbf{h}_k$, $1 \leq n \leq N_h$). Consequently, the differential modulation can be performed by using the Mixed Domain Scheme (MDS) [23], where the differential data can be simultaneously encoded in both time and frequency domains. The main benefit of this scheme is that only two reference signals are required for transmission of a total of N_h OFDM symbols (KN_h resources), reducing further the overhead as compared to the FDS.

Firstly, the data symbols are differentially encoded as

$$\tilde{x}_i = \begin{cases} p_i, & i = 1 \\ \tilde{x}_{i-1} p_i, & i = 2 \\ \tilde{x}_{i-1} s_i, & 3 \leq i \leq KN_h \end{cases}, \tag{11}$$

where the i denotes the resource index. Then, the differential symbols $\tilde{x}_i$ are allocated to the two-dimensional resource grid as

$$x_{k,n} = \tilde{x}_i \mid (k,n) = f(i), \quad 1 \leq i \leq KN_h, \tag{12}$$

where $f(\cdot)$ is the resource mapping policy function. A possible mapping policy is given in [23], which mainly follows the FDS, except for the edge subcarriers of the block, that follow a Time-Domain Scheme (TDS). The latter consists on performing the differential encoding using resources of the same subcarrier at two consecutive OFDM symbols.

Similarly to the previous stage, the residual phase compensation is also required, except for those differential symbols following the TDS. The residual phase component for the second stage (ζ_h) can be estimated by using only the first two subcarriers of the first OFDM symbol as follows:

$$\widehat{\zeta}_h = \measuredangle \left(\left(\mathbf{y}_{1,1} \right)^H \mathbf{y}_{2,1} \right) - \measuredangle \left(\frac{p_{2,1}}{p_{1,1}} \right). \tag{13}$$

IV. Throughput and Complexity Comparison

In this section, a comparison in terms of throughput and complexity among the proposed NCDS and the baseline cases are given, in order to show the superiority of the NCDS.

For the first stage of beam training, two baseline approaches are taken into account for comparison purposes. The transmitted symbols can be either exclusively Reference Signals (RS) [15], or the traditional CDS (pilot and data symbols). Therefore, the main difference between these two cases is that CDS is also able to transmit some information. The chosen combiner for this stage is Maximum Ratio Combining (MRC) since the channel gain of the direct link is not very high.

For the second stage, only the classical CDS is considered. According to [16], the first OFDM symbol of this stage is exclusively employed for channel estimation, while the $N_h - 1$ OFDM symbols left are used for data transmission. Unlike the first stage, the chosen combiner is Zero-Forcing (ZF) since the channel gain of the reflected link is enhanced by the RIS, and for high-SINR ZF is superior to MRC.

A. Throughput Comparison

For a typical packet-based transmission, the total throughput of the system can be defined as $R = R_l + R_h$ [packet/s], where R_l and R_h refer to the throughput of the first and second stages, respectively. Similarly to [24], the throughput of each stage can be found as

$$R_l = \eta_l \frac{\Delta f K}{L_P} \left(1 - P_{e,l}\right)^{L_P} \log_2(Q_l), \tag{14}$$

$$R_h = \eta_h \frac{\Delta f K}{L_P} \left(1 - P_{e,h}\right)^{L_P} \log_2(Q_h), \tag{15}$$

where $P_{e,l}$ and $P_{e,h}$ are the BER for the two stages, Q_l and Q_h are the constellation sizes of each stage, L_P denotes the number of bits in one packet, and η_l and η_h are the efficiency of the system for the two stages, taking into account the overhead from the transmission of the reference signals.

TABLE I
Complexity Comparison between the Proposed NCDS and the Considered Baseline RS and CDS.

	RS	CDS	NCDS
Stage One	0	$N_l \left(BK_p + B^2 \left(K - K_p \right) + C_I \right)$	$2\left(K-1\right) N_l$
Stage Two	-	$BK \left(\left(B^2 + 1 \right) + B \left(N_h - 1 \right) \right)$	$2\left(KN_h - 1\right)$

The efficiency of the first stage is given by

$$\eta_l = N_l \left(K - K_p \right) / NK, \tag{16}$$

where K_p is the number of reference symbols at each OFDM symbol. For the CDS scenario, the number of pilot symbols is typically a portion of the total amount of subcarriers ($K_p < K$). On the other hand, the pilot-based approach and the proposed NCDS are two particular cases of (16), where the number of reference signals is fixed to $K_p = K$ and $K_p = 2$, respectively.

After the best phase configuration is chosen, the data transmission is enhanced by the RIS. The efficiency of this second stage for the CDS and NCDS cases are

$$\eta_h^{\text{CDS}} = \frac{N_h - 1}{N}, \quad \eta_h^{\text{NCDS}} = \frac{N_h K - 2}{NK}, \tag{17}$$

respectively, where one OFDM symbol is used for channel estimation for the CDS. On the contrary, only two reference symbols placed at the first OFDM symbol are required out of N_h OFDM symbols for NCDS.

Taking into account (**??**), the proposed NCDS for both stages is capable of outperforming the classical CDS, especially for high mobility scenarios, since it does not require to transmit a large amount of reference signals, and its efficiency is not degraded ($\eta_h^{\text{NCDS}} \to 1$).

B. Complexity Comparison

The complexity evaluation is performed accounting for the number of required complex product operations for each case, which are summarized in Table I, specifically the procedures related to channel estimation and equalization at the BS for a chosen codeword. Note that the operations needed for measuring the energy in order to determine the best beam at RIS are not considered in the stage one for this comparison, since they are the same for all approaches.

For the first stage, RS does not require any additional operations due to the fact that it does not transmit any data symbols. On the contrary, CDS is transmitting both data and pilot symbols, and hence, it has to estimate the channel and perform a MRC equalization for each OFDM symbol. Note that the computation of the MRC combiner is neglected, since it is obtained by performing a complex conjugate of the estimated channel. Additionally, the channel estimates at the pilot symbol resources must be interpolated to obtain values for the data resources. The complexity of this interpolation is given by C_I, and this value depends on the chosen algorithm [25]. However, the proposed NCDS only performs the differential

TABLE II
SIMULATION PARAMETERS

BS location	(0,0,3)	$\mathbf{f_c}$	3.5 GHz	**K**	1024
RIS location	(10,0,3)	**Δf**	30 KHz	$\boldsymbol{\sigma_v^2}$	-90 dBW
UE location	(10,12,1)	$\mathbf{L_d}$	-86 dB	**B**	4×4
Mod. NCDS	4, 16-PSK	$\mathbf{L_u}$	-50 dB	**M**	8×8
Mod. CDS	4, 16-QAM	$\mathbf{L_u}$	-52 dB	$\mathbf{N_l}$	140

encoding and decoding $K-1$ times for each OFDM symbol. For the second stage, the classical CDS performs the channel estimation and computation of the ZF combiner at the first OFDM symbol, which requires a matrix inversion. Then, the remaining OFDM data symbols are equalized. Again, the NCDS only requires the differential encoding and decoding operations.

The proposed NCDS has less complexity in terms of complex products as compared to the traditional CDS, since channel estimation, computation of the combiner, and the equalization operations are not required. Moreover, the classical CDS not only requires more computations, but it also needs more memory to store the channel estimation samples and the computed combiners. Consequently, the proposed NCDS system is cost-effective and/or able to reduce the delay of the communication system.

V. PERFORMANCE EVALUATION RESULTS

In this section, numerical results are provided to show the performance of the proposed NCDS, as compared to the considered baseline cases presented in the previous section. For a more realistic performance evaluation, all the links (BS-UE, BS-RIS and RIS-UE) are generated according to the 5G standard [6]. The channel propagation model adopted for the simulation results corresponds to the 3GPP factory scenario of size (60m,120m,3m). Moreover, a summary of the simulation parameters is provided in Table II, the location of each network node is given by the Cartesian coordinates (x, y, z) measured in meters, and f_c denotes the carrier frequency. The distance between any two contiguous elements of the BS and RIS is set to half wavelength ($d_H^{\text{BS}} = d_V^{\text{BS}} = d_H^{\text{RIS}} = d_V^{\text{BRIS}} = \lambda/2$). Additionally, to show the quality of the phase configuration based on codeword selection, the performance provided by the best configuration (i.e., upper-bound) is also shown.

The BER comparison between the classical CDS and the proposed NCDS signaling is depicted in Fig. 2. For the stage one, the chosen modulation is 4-QAM and 4-PSK for the CDS and NCDS, respectively, and the selected equalization technique for CDS is MRC. For the second stage, the chosen modulation is 16-QAM and 16-PSK for the CDS and NCDS, respectively, and the selected equalization technique for CDS is ZF. Even though the CDS is able to outperform the NCDS in terms of BER, this result does not account for the time/frequency and energy resources required for the transmission of reference signals (efficiency) and the complexity described in Section IV. Moreover, the degradation produced by the CDS is higher than NCDS for the particular case of codeword selection. The reason behind this behavior is

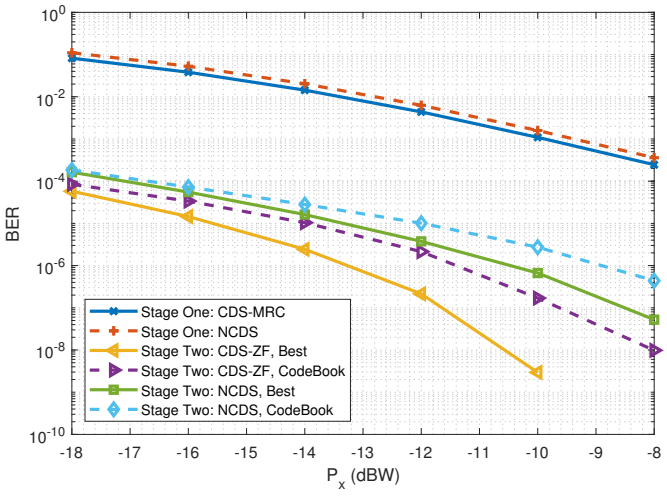

Fig. 2. BER comparison between CDS and NCDS for both stages.

due to the fact that CDS requires accurate channel estimates, especially for the particular case of ZF criterion. Otherwise, the computed equalizers will enhance the noise.

A throughput comparison is shown taking into account the configurations described in Section IV. The constellation sizes are $Q_l = 4$ and $Q_h = 16$, the packet length is set to $L_P = 20$, and for the particular case of CDS at the stage one, the ratio of pilot symbols transmitted at each OFDM symbol is set to $K/K_p = 3$. In Table III, the throughput is evaluated for both stages at different values of speed for the UE, which is equivalent to evaluating the performance at several values of channel coherence times (T_c) and their corresponding lengths (N), taking into account the OFDM numerology given in Table II. On the one hand, the NCDS is always outperforming the CDS in the first stage, as a result of avoiding the reference signals in order to track the strongly time-varying channels produced by the RIS. Moreover, the throughput of the CDS is slightly lower than the NCDS in the second stage, since the additional OFDM symbol spent for channel estimation becomes negligible. On the other hand, comparing the throughput produced by the two stages, the proposed NCDS scheme contributes more to the total throughput (R) as compared to the CDS, especially when the channel coherence time or the number of total OFDM symbols is not large. For example, for the case of 7.3 m/s ($N = N_l$), the NCDS can double the throughput.

In Fig. 3, the total throughput (R) is shown for the different baseline cases described in the previous section. The two bottom curves represent the total throughput for the case of exclusively transmitting reference signals at the beam-training case, while both CDS and NCDS are exploited at the second stage. Note that the NCDS slightly outperforms the CDS due to the fact that the latter requires an additional OFDM symbol for transmitting the reference signals for channel estimation. Then, the proposed fully NCDS system has a significant higher throughput as compared to the fully CDS one, since the NCDS is capable of transmitting more data symbols at the first stage, where no reference signals are needed.

TABLE III
THROUGHPUT COMPARISON BETWEEN CDS AND NCDS AT EACH STAGE FOR $P_x = -8$ DB IN [10^6 PACKETS/S].

	7.3 m/s $N = N_l$		4.8 m/s $N = 1.5N_l$		3.6 m/s $N = 2N_l$		2.4 m/s $N = 3N_l$	
Stage	One	Two	One	Two	One	Two	One	Two
CDS	2.04	0	1.36	2.04	1.02	3.06	0.68	4.09
NCDS	3.05	0	2.04	2.05	1.53	3.07	1.02	4.1

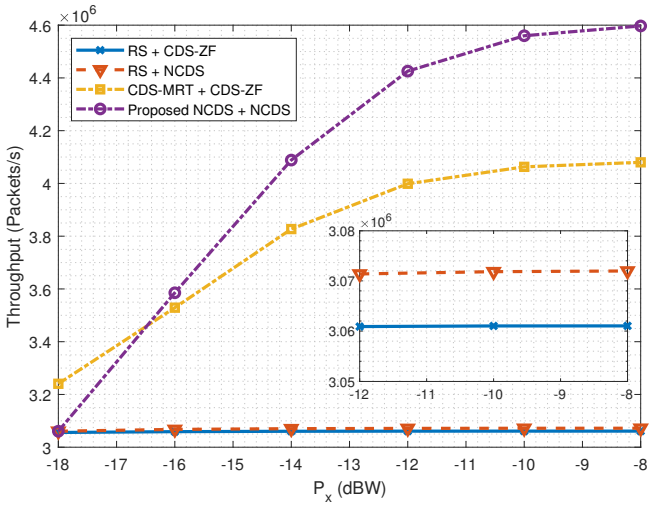

Fig. 3. Throughput comparison between CDS and NCDS for a speed of 4 m/s, which corresponds to $N = 2N_l$.

VI. CONCLUSIONS

This paper investigated NCDS based on differential modulation, which was adequately combined with a codebook-based beam training for the RIS. The proposed scheme is able to execute the beam training process at the RIS, while at the same time, transmitting differential data symbols through the direct and reflective links, where the latter is strongly time-varying as a consequence of beam training. Therefore, this combination is able to efficiently obtain the best phase configuration for the RIS and increase the data-rate of the system, especially in scenarios with moderate-to-high mobility and/or a highly attenuated direct BS-UE link. The proposed method is simple, yet effective, as compared to conventional RIS-empowered systems based on CDS. The presented analysis for the efficiency and complexity revealed that the proposed NCDS requires a substantially smaller amount of reference signals and complex products. Hence, these additional benefits will reduce the cost, energy consumption, and latency of the system.

ACKNOWLEDGMENTS

This work has been funded by the Spanish National project IRENE-EARTH (PID2020-115323RB-C33/AEI /10.13039/501100011033) and the EU H2020 RISE-6G project under grant number 101017011.

REFERENCES

[1] C. Huang, A. Zappone *et al.*, "Reconfigurable intelligent surfaces for energy efficiency in wireless communication," *IEEE Trans. Wireless Commun.*, vol. 18, no. 8, pp. 4157–4170, Aug. 2019.

[2] C. Liaskos, S. Nie *et al.*, "A new wireless communication paradigm through software-controlled metasurfaces," *IEEE Commun. Mag.*, vol. 56, no. 9, pp. 162–169, Sep. 2018.

[3] M. Di Renzo, M. D. D.-T. Phan-Huy *et al.*, "Smart radio environments empowered by reconfigurable AI meta-surfaces: an idea whose time has come," *EURASIP J. Wireless Commun. Net.*, vol. 2019, no. 1, pp. 1–20, May 2019.

[4] E. C. Strinati, G. C. Alexandropoulos *et al.*, "Reconfigurable, intelligent, and sustainable wireless environments for 6G smart connectivity," *IEEE Commun. Mag.*, vol. 59, no. 10, pp. 99–105, Oct. 2021.

[5] "The next hyper-connected experience for all," White Paper, Samsung 6G Vision, Jun. 2020.

[6] "Study on channel model for frequencies from 0.5 to 100 GHz (Release 17)," 3GPP, France, Technical Report 38.901, 2022.

[7] T. L. Jensen and E. De Carvalho, "An optimal channel estimation scheme for intelligent reflecting surfaces based on a minimum variance unbiased estimator," in *Proc. IEEE ICASSP*, Barcelona, Spain, May 2020, pp. 5000–5004.

[8] Z. He and X. Yuan, "Cascaded channel estimation for large intelligent metasurface assisted massive MIMO," *IEEE Wireless Commun. Lett.*, vol. 9, no. 2, pp. 210–214, Feb. 2020.

[9] H. Liu, X. Yuan, and Y. A. Zhang, "Matrix-calibration-based cascaded channel estimation for reconfigurable intelligent surface assisted multiuser MIMO," *IEEE J. Sel. Areas Commun.*, vol. 38, no. 11, pp. 2621–2636, Nov. 2020.

[10] C. You, B. Zheng, and R. Zhang, "Channel estimation and passive beamforming for intelligent reflecting surface: Discrete phase shift and progressive refinement," *IEEE J. Sel. Areas Commun.*, vol. 38, no. 11, pp. 2604–2620, Nov. 2020.

[11] Q. U. A. Nadeem, H. Alwazani *et al.*, "Intelligent reflecting surface-assisted multi-user MISO communication: Channel estimation and beamforming design," *IEEE Open J. Commun. Society*, vol. 1, pp. 661–680, May 2020.

[12] B. Zheng and R. Zhang, "Intelligent reflecting surface-enhanced OFDM: Channel estimation and reflection optimization," *IEEE Wireless Commun. Lett.*, vol. 9, no. 4, pp. 518–522, Apr. 2020.

[13] M. Najafi, V. Jamali *et al.*, "Physics-based modeling and scalable optimization of large intelligent reflecting surfaces," *IEEE Trans. Commun.*, vol. 69, no. 4, pp. 2673–2691, Apr. 2021.

[14] C. Huang, G. C. Alexandropoulos *et al.*, "Energy efficient multi-user MISO communication using low resolution large intelligent surfaces," in *Proc. IEEE GLOBECOM*, Abu Dhabi, UAE, Dec. 2018, pp. 1–6.

[15] C. You, B. Zheng, and R. Zhang, "Fast beam training for IRS-assisted multiuser communications," *IEEE Wireless Commun. Lett.*, vol. 9, no. 11, pp. 1845–1849, 2020.

[16] V. Jamali, G. C. Alexandropoulos *et al.*, "Low-to-zero-overhead IRS reconfiguration: Decoupling illumination and channel estimation," *IEEE Commun. Lett.*, vol. 26, no. 2, pp. 932–936, Apr. 2022.

[17] C. Psomas and I. Krikidis, "Low-complexity random rotation-based schemes for intelligent reflecting surfaces," *IEEE Trans. Wireless Commun.*, vol. 20, no. 8, pp. 5212–5225, Aug. 2021.

[18] K. Chen-Hu, G. C. Alexandropoulos, and A. G. Armada, "Non-coherent MIMO-OFDM uplink empowered by the spatial diversity in reflecting surfaces," in *Proc. IEEE WCNC*, Austin, USA, Apr. 2022.

[19] G. C. Alexandropoulos, I. Vinieratou *et al.*, "Uplink beam management for millimeter wave cellular MIMO systems with hybrid beamforming," in *Proc. IEEE WCNC*, Nanjing, China, Apr. 2021, pp. 1–7.

[20] A. G. Armada and L. Hanzo, "A non-coherent multi-user large scale SIMO system relaying on M-ary DPSK," in *Proc. IEEE ICC*, June 2015, pp. 2517–2522.

[21] K. Chen-Hu and A. G. Armada, "Non-coherent multiuser massive MIMO-OFDM with differential modulation," in *Proc. IEEE ICC*, May 2019, pp. 1–6.

[22] K. Chen-Hu, Y. Liu, and A. G. Armada, "Non-coherent massive MIMO-OFDM down-link based on differential modulation," *IEEE Trans. Veh. Technol.*, vol. 69, no. 10, pp. 11 281–11 294, Oct. 2020.

[23] K. Chen-Hu, Y. Liu, and A. G. Armada, "Non-coherent massive MIMO-OFDM for communications in high mobility scenarios," *ITU J. Future and Evolving Technol.*, vol. 1, no. 1, pp. 13–24, Nov. 2020.

[24] M. J. Lopez-Morales, K. Chen-Hu, and A. Garcia-Armada, "Differential data-aided channel estimation for up-link massive SIMO-OFDM," *IEEE Open J. of the Commun. Society*, vol. 1, pp. 976–989, Jul. 2020.

[25] X. Dong, W.-s. Lu, and A. C. Soong, "Linear interpolation in pilot symbol assisted channel estimation for OFDM," *IEEE Trans. Wireless Commun.*, vol. 6, no. 5, pp. 1910–1920, May 2007.